

Electrodynamic Structure of an Outer-Gap Accelerator: Upper Limits of Pulsed TeV Emissions from the Crab Pulsar

Kouichi Hirotani

Code 661, Lab. for High-Energy Astroph., NASA/GSFC, Greenbelt, MD 20771, U.S.A.

Shinpei Shibata

Department of Physics, Yamagata University, Yamagata 990-8560, Japan

We investigate a stationary pair production cascade in the outer magnetosphere of a spinning neutron star. The charge depletion caused by global flows of charged particles, exerts a large electric field along the magnetic field lines. Migratory electrons and/or positrons are accelerated by this field to radiate curvature gamma-rays, some of which collide with the X-rays to materialize as pairs in the gap. The replenished charges partially screen the electric field, which is self-consistently solved together with the distribution functions of particles and gamma-rays. If no current is injected at either of the boundaries of the accelerator, the gap is located around the null surface, where the local Goldreich-Julian charge density vanishes. However, we first find that the gap position shifts outwards (or inwards) when particles are injected at the inner (or outer) boundary. Applying the theory to the Crab pulsar, we demonstrate that the gap should be located near to or outside of the null surface so that the expected spectrum may be consistent with EGRET observations and that the pulsed TeV flux does not exceed the observational upper limits for moderate infrared photon density.

1 Introduction

The EGRET experiment on the Compton Gamma Ray Observatory has detected pulsed signals from seven rotation-powered pulsars (e.g., for Crab, Nolan et al. 1993, Fierro et al. 1998). The modulation of the γ -ray light curves at GeV energies testifies to the production of γ -ray radiation in the pulsar magnetospheres either at the polar cap (Harding, Tademaru, & Esposito 1978; Daugherty & Harding 1982, 1996; Sturmer, Dermer, & Michel 1995; Shibata, Miyazaki, & Takahara 1998), or at the vacuum gaps in the outer magnetosphere (Cheng et al. 1986a,b, hereafter CHR; Chiang & Romani 1992, 1994; Romani 1996; Zhang & Cheng 1997; Cheng et al. 2000). Effective γ -ray production in a pulsar magnetosphere may be extended to the very high energy (VHE) region above 100 GeV as well; however, the predictions of fluxes by the current models of γ -ray pulsars are not sufficiently conclusive. Whether or not the spectra of γ -ray pulsars continue up to the VHE region is a question that remains one of the interesting issues of high-energy astrophysics.

In the VHE region, positive detections of radiation at a high confidence level have been reported from the direction of the Crab pulsar (Nel et al. 1993). However, as for *pulsed* TeV radiation, only the upper limits have been, as a rule, obtained (Akerlof et al. 1993; Borione et al. 1997; Srinivasan et al. 1997; Yoshikoshi et al. 1997; Sako et al. 2000; de Naurois et al. 2002). If the VHE emission originates in the pulsar magnetosphere, a significant fraction of it can be expected to show pulsation. Therefore, the lack of *pulsed* TeV emissions provides a severe

constraint on the modeling of particle acceleration zones in a pulsar magnetosphere.

In fact, in the CHR picture, the magnetosphere should be optically thick for pair-production in order to reduce the TeV flux to an unobserved level by absorption. This in turn requires very high luminosities of infrared photons. However, the required IR fluxes are generally orders of magnitude larger than the observed values (Usov 1994). We are therefore motivated by the need to contrive an outer-gap model that produces less TeV emission with a moderate infrared luminosity.

High-energy emission from a pulsar magnetosphere, in fact, crucially depends on the acceleration electric field, E_{\parallel} , along the magnetic field lines. It was Hirotani and Shibata (1999a,b,c; hereafter Papers I, II, III) who first considered the spatial distribution of E_{\parallel} together with particle and γ -ray distribution functions. By solving these Vlasov equations, they demonstrated that a stationary gap is formed around the null surface at which the local Goldreich-Julian charge density,

$$\rho_{\text{GJ}} = -\frac{\Omega B_z}{2\pi c}, \quad (1)$$

vanishes, where B_z is the component of the magnetic field along the rotation axis, Ω the angular frequency of the neutron star, and c the speed of light. Equation (1) is valid unless the gap is located close to the light cylinder, of which distance from the rotation axis is given by $\varpi_{\text{LC}} = c/\Omega$. In the present paper, we apply this theory to the Crab pulsar and discuss the γ -ray emission properties as a function of the gap position, which is determined by the magnetospheric current.

In the next two sections, we describe the physical processes of pair production cascade and the resultant γ -ray emission. Applying the theory to the Crab pulsar, we present expected γ -ray spectra and flux in § 3.

2 Basic Equations and Boundary Conditions

2.1 The Vlasov Equations

We simply assume that the electrostatic and the curvature-radiation-reaction forces cancel each other in the Boltzmann equations of particles. Under this mono-energetic approximation, the Boltzmann equations reduce to continuity equations. Assuming that the toroidal bending is negligible for the magnetic field, we obtain the following stationary ($\partial_t + \Omega\partial_\phi = 0$) continuity equations (Hirotani & Shibata 2001ab, 2002, Paper VII,VIII,IX),

$$\pm B \frac{d}{ds} \left(\frac{N_{\pm}}{B} \right) = \frac{1}{c} \int_0^\infty d\epsilon_\gamma [\eta_{\text{p}+} G_+ + \eta_{\text{p}-} G_-], \quad (2)$$

where N_+ and N_- represent the spatial densities of positrons and electrons, respectively, G_+ and G_- the distribution functions of outwardly and inwardly propagating γ -rays, respectively, and B the strength of the magnetic field; $\eta_{\text{p}+}$ (or $\eta_{\text{p}-}$) refers to the pair production rate for a curvature-radiated γ -ray photon propagating outwards (or inwards) per unit length.

A combination of equations (2) gives the current conservation law,

$$j_{\text{tot}} \equiv \frac{2\pi ce}{\Omega} \left[\frac{N_+(s)}{B(s)} + \frac{N_-(s)}{B(s)} \right] = \text{constant for } s. \quad (3)$$

If $j_{\text{tot}} = 1$ holds, the current density per unit magnetic flux tube equals the Goldreich-Julian value, $\Omega/(2\pi)$.

Let us next consider the γ -ray Boltzmann equations. We assume that the outwardly (or inwardly) propagating γ -rays dilate (or constrict) at the same rate with the magnetic field; this assumption gives a good estimate when $W \ll \varpi_{\text{LC}}$ holds. We then obtain the following two

equations

$$\pm cB \frac{\partial}{\partial s} \left(\frac{G_{\pm}}{B} \right) = -\eta_{p\pm} G_{\pm} + \eta_c N_{\pm}, \quad (4)$$

where η_c refers to the curvature radiation rate.

We finally consider the Poisson equation for the electrostatic potential. Assuming that the transfield thickness of the gap is greater than W , we can reduce the Poisson equation into one dimension as (Paper VII)

$$E_{\parallel} = -\frac{d\psi}{ds}, \quad \frac{dE_{\parallel}}{ds} = 4\pi e \left(N_+ - N_- - \frac{\rho_{\text{GJ}}}{e} \right) \quad (5)$$

We compute Γ , particle Lorentz factor, at each point s , by balancing the electrostatic acceleration and the curvature-radiation-reaction force.

2.2 Boundary Conditions

To solve the Vlasov equations (2), (5), and (4), we consider the boundary conditions. At the *inner* (starward) boundary ($s = s_1$), we impose (Paper VII)

$$E_{\parallel}(s_1) = 0, \quad \psi(s_1) = 0, \quad G_+(s_1) = 0 \quad \frac{N_+(s_1)}{B(s_1)} = j_1 \frac{\Omega}{2\pi c e}. \quad (6)$$

If $j_1 = 0$, positronic current injection equals the Goldreich-Julian value. Note that equations (3) and (6) yield

$$N_-(s_1) = j_{\text{tot}} - j_1. \quad (7)$$

At the *outer* boundary ($s = s_2$), we impose

$$E_{\parallel}(s_2) = 0, \quad G_-(s_2) = 0, \quad \frac{N_-(s_2)}{B(s_1)} = j_2 \frac{\Omega}{2\pi c e}. \quad (8)$$

The current density created in the gap per unit flux tube can be expressed as

$$j_{\text{gap}} = j_{\text{tot}} - j_1 - j_2. \quad (9)$$

We adopt j_{gap} , j_1 , and j_2 as the free parameters.

Dividing the γ -ray energies into $m (= 11)$ bins, we obtain $2m + 6$ boundary conditions (6)–(8) for $2m + 4$ unknown functions Ψ , E_{\parallel} , N_{\pm} , g_{\pm}^i ($i = 1, 2, \dots, m$), where g_{\pm}^i refers to G_{\pm} integrated in each energy bin. Thus two extra boundary conditions must be compensated by making both of the boundaries s_1 and s_2 be free. The two free boundaries appear because $E_{\parallel} = 0$ is imposed at *both* the boundaries and because j_{gap} is externally imposed. In other words, a gap changes its position if j_1 and/or j_2 varies.

3 Application to the Crab Pulsar

3.1 Input X-ray and Infrared Field

To evaluate the pair-production rate $\eta_{p\pm}$, we must specify the X-ray density and spectrum. We adopt the following HEAO 1 observations in the primary pulse phase:

$$\frac{dN_{\text{pl}}}{d\epsilon_x} = N_{\text{pl}} \epsilon_x^{-\alpha} \quad (\epsilon_{\text{min}} < \epsilon_x < \epsilon_{\text{max}}), \quad (10)$$

where $\alpha = -1.81$ and $N_{\text{pl}} = 5.3 \times 10^{15} (d/\text{kpc})^2 (r_{\text{cnt}}/\varpi_{\text{LC}})^{-2}$ (Knight 1982). We adopt $\epsilon_{\text{min}} = 0.1\text{keV}/511\text{keV}$ and $\epsilon_{\text{max}} = 50\text{keV}/511\text{keV}$.

To investigate the TeV flux, we must evaluate the IR field illuminating the gap. It should be noted that the optical depth for a TeV photon to be absorbed by colliding with one of the IR photons is greater than unity for the Crab pulsar (e.g., fig. 3 in Paper VII). Therefore, to examine the conservative upper limit of pulsed TeV flux, we must consider the IR field as small as possible. To this end, we assume that the IR photons are self-absorbed and sharply decrease below $\epsilon_{\text{IR}} < 10^{-6}$ (or equivalently, below 1.23×10^{14} Hz). Assuming an isotropic IR field within a uniform sphere of radius ϖ_{LC} , we obtain the following flux density at distance d :

$$F_{\nu} = \frac{c}{4} \left(\frac{\varpi_{\text{LC}}}{d} \right)^2 h N_0 \epsilon_{\text{IR}}^{\alpha+1} = 4.5 \times 10^{-20} \Omega_2^{-2} \left(\frac{d}{\text{kpc}} \right)^{-2} \epsilon_{\text{IR}} \frac{dN_{\text{IR}}}{d\epsilon_{\text{IR}}} \quad \text{Jy}; \quad (11)$$

for a power-law spectrum. Therefore, the IR photon density per dimensionless energy $\epsilon_{\text{IR}} \equiv h\nu/m_e c^2$, becomes

$$\frac{dN_{\text{IR}}}{d\epsilon_{\text{IR}}} = N_0 \epsilon_{\text{IR}}^{\alpha}. \quad (12)$$

Setting $F_{\nu} = 3$ mJy at $\epsilon_{\text{IR}} = 10^{-6}$, which is consistent with near-IR and optical observations (Eikenberry et al. 1997), we obtain $N_0 = 2.3 \times 10^{32} \text{cm}^{-3}$ and $\alpha = -0.88$ for $\epsilon_{\text{IR}} > 10^{-6}$ (and of course $\alpha = 1.5$ for $\epsilon_{\text{IR}} < 10^{-6}$).

3.2 Results

We apply the theory to the Crab pulsar, whose rotational frequency and the magnetic moment are 188.1rad s^{-1} and $3.38 \times 10^{30} \text{G cm}^3$. First, let us investigate the spatial distribution of the acceleration field. We consider the following three representative boundary conditions:

case 1 $(j_1, j_2) = (0, 0) \rightarrow$ solid curve in figures 1 (left and right),

case 2 $(j_1, j_2) = (0.25, 0) \rightarrow$ dashed curve,

case 3 $(j_1, j_2) = (0.50, 0) \rightarrow$ dash-dotted curve.

For example, for case 2, the positronic current density flowing into the gap per unit flux tube at the inner boundary is 25% of the typical Goldreich-Julian value, $\Omega/2\pi$. In what follows, we adopt 45° as the magnetic inclination.

The results of $E_{\parallel}(s)$ for the three cases are presented in figure 1 (left). The abscissa designates the distance along the last-open field line and covers the range from the neutron star surface ($s = 0$) to the position where the distance equals $s = 1.3\varpi_{\text{LC}} = 2.07 \times 10^6$ m.

The solid curve (case 1) shows that the gap is located around the null surface if there is no particle injection across either of the boundaries. However, the gap shifts outwards as j_1 increases, as the dashed (case 2) and dash-dotted (case 3) curves indicate. Moreover, the accelerator is localized in the outer magnetosphere; the typical width is only 5 % of ϖ_{LC} . For case 1, E_{\parallel} exceeds 10^9 V/m, which is about 10 times greater than previously assumed values. Such a localized structure arises from the fact that the strong X-ray field of this young pulsar results in a short pair-production mean-free path and hence the spatial extent of the gap.

Let us next consider the GeV and TeV spectrum. We adopt the cross sectional area of $D_{\perp}^2 = (6W)^2$ for all the cases to be considered, so that the GeV flux in cases 1 and 2 may be consistent with observations. If D_{\perp} increase twice, both the GeV and TeV fluxes increases four times.

For the three different boundary conditions (cases 1, 2, and 3), the spectra of the outwardly propagating γ -rays, of which flux dominates that of the inwardly propagating ones in each case, are presented in figure 1 (right). In GeV energies, the observational pulsed spectrum is obtained by EGRET observations (open circles; Nolan et al. 1993), while in TeV energies, only the upper limits are obtained by Whipple observations (open squares; Weekes et al. 1989; Reynolds et al.

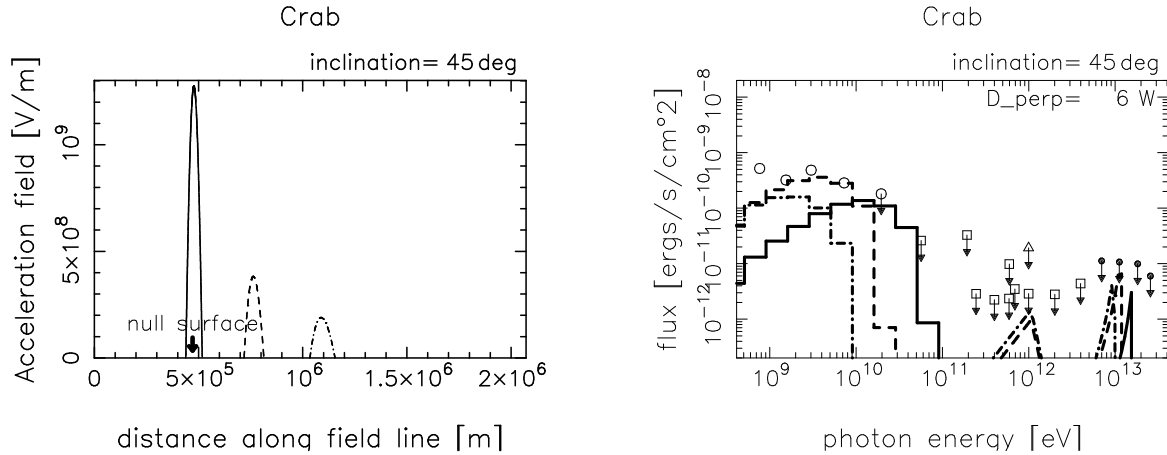


Figure 1: **(Left)** Distribution of $E_{\parallel}(s)$ for the Crab pulsar with $\alpha_i = 45^\circ$; the abscissa is in meters. The solid, dashed, dash-dotted curves correspond to the cases 1, 2, 3, respectively (see text). **(Right)** Expected curvature (GeV) and inverse-Compton (TeV) spectra for each case; observed, pulsed spectrum is also plotted.

1993; Goret et al. 1993; Hillas, A. M.; Lessard et al. 2000), Durham observations (open triangle; Douthwaite et al. 1984), and CELESTE observations (open square at 60 GeV; de Naurois et al. 2002). The filled circles denote the unpulsed flux obtained by CANGAROO observations (Tanimori et al. 1998).

So that the GeV emission may be consistent with EGRET observations, the gap should be geometrically thick in the transfield direction ($D_{\perp} = 6W$). For this cross-sectional area, pulsed TeV flux is kept below the observational upper limits.

In summary, we have developed a one-dimensional model for an outer-gap accelerator in the magnetosphere of a rotation-powered pulsar. When particles flow into the gap across the outer (or inner) boundary, the gap shifts inwards (or outwards). Applying this method to the Crab pulsar, we find that the gap is localized in the outer magnetosphere because of the dense X-ray field of this young pulsar. In spite of this limited spatial extent, the gap produces significant GeV emissions, because its strong acceleration field (10^9V m^{-1}) results in a sufficient potential drop (10^{14}V). However, the TeV flux is suppressed below the observed upper limits, because the efficiency of inverse-Compton scatterings does not strongly depend on the particle Lorentz factors, which is closely related with the acceleration field strength, compared with that of curvature process.

Acknowledgments

One of the authors (K. H.) wishes to express his gratitude to Dr. A. K. Harding for valuable advice.

References

1. Akerlof, C. W. et al. 1993, A& A 274, L17
2. Borione, A., Catanese, M. A., Chantell, M. C., Covault, C. E., Cronin, J. W., Fick, B. E., Fortson, L. F., Fowler, J. F. et al. 1997, ApJL 481, L 313
3. Cheng, K. S., Ho, C., Ruderman, M., 1986a ApJ, 300, 500
4. Cheng, K. S., Ho, C., Ruderman, M., 1986b ApJ, 300, 522
5. Chiang, J., Romani, R. W. 1992, ApJ, 400, 629
6. Cheng, K. S., Ruderman, M., Zhang, L. 2000, ApJ, 537, 964

7. Chiang, J., Romani, R. W. 1994, *ApJ*, 436, 754
8. Daugherty, J. K., Harding, A. K. 1982, *ApJ*, 252, 337
9. Daugherty, J. K., Harding, A. K. 1996, *ApJ*, 458, 278
10. de Naurois et al. 2002, *ApJ*, 566, 343
11. Dowthwaite, J. C., et al. 1984, *ApJ* 286, L35
12. Eikenberry, S. S., Fazio, G. G., Ransom, S. M., Middleditch, J., Kristaian, J., Pennypacker, C. R. 1997, *ApJ* 477, 465
13. Harding, A. K., Tadamaru, E., Esposito, L. S. 1978, *ApJ*, 225, 226
14. Fierro, J. M., Michelson, P. F., Nolan, P. L., Thompson, D. J., 1998, *ApJ* 494, 734
15. Goret, P., Palfey, T., Tabary, A., Vacanti, G., Bazer-Bachi, R. 1993, *A&A* 270, 401
16. Hillas, A. M., Akerlof, C. W., Biller, S. D., Buckley, J. H., Carter-Lewis, D. A., Catanese, M., Cawley, M. F., Fegan, D. J. et al. 1998, *ApJ* 503, 744
17. Hirotani, K. Shibata, S., 1999a, *MNRAS* 308, 54 (Paper I)
18. Hirotani, K. Shibata, S., 1999b, *MNRAS* 308, 67 (Paper II)
19. Hirotani, K. Shibata, S., 1999c, *PASJ* 51, 683 (Paper III)
20. Hirotani, K. Shibata, S., 2001a, *Astroph. J.* 558, 216 (Paper VII)
21. Hirotani, K. Shibata, S., 2001, *MNRAS* 325, 1228 (Paper VIII)
22. Hirotani, K. Shibata, S. 2002, *Astrophys. J.*, 564, 369 (Paper IX)
23. Knight F. K. 1982, *ApJ* 260, 538
24. Lessard, R. W., Bond, I. H., Bradbury, S. M., Buckley, J. H., Burdett, A. M., Carter-Lewis, D. A. Catanese, M. Cawley, M. F., et al. 2000, *ApJ* 531, 942
25. Nel, H. I., De Jager, O. C., Raubenheimer, B. C., Brink, C., Meintjes, P. J., Nortt, A. R. 1993, *ApJ* 418, 836
26. Nolan, P. L., Arzoumanian, Z., Bertsch, D. L., Chiang, J., Fichtel, C. E., Fierro, J. M., Hartman, R. C., Hunter, S. D., et al. 1993, *ApJ* 409, 697
27. Reynolds, P. T., et al., 1993, *ApJ* 404, 206
28. Romani, R. W. 1996, *ApJ*, 470, 469
29. Sako, T., Matsubara, Y., Muraki, Y., Ramanamurthy, R. V., Dazeley, S. A., Edwards, P. G., Gunji, S., Hara, T. et al. 2000, *ApJ* 537, 422
30. Shibata, S., Miyazaki, J., Takahara, F. 1998, *MNRAS* 295, L53
31. Srinivasan, R. et al. 1997, *ApJ* 489, 170
32. Sturmer, S. J., Dermer, C. D., Michel, F. C. 1995, *ApJ* 445, 736
33. Tanimori et al. 1998, *ApJ* 492, L33
34. Usov, V. V. 1994, *ApJ* 427, 394
35. Weekes, T. C., et al. 1989, *ApJ* 342,379
36. Yoshikoshi, T., Kifune, T., Dazeley, S. A., Edwards, P. G., Hara, T., Hayami, Y., Kikimoto, F., Konishi, T. 1997, *ApJ* 487, L65
37. Zhang, L. Cheng, K. S. 1997, *ApJ* 487, 370